

Temperature-induced phase transition of two-dimensional semiconductor GaTe

Xiaoyu Wang(王啸宇), Xue Wang(王雪), Hongshuai Zou(邹洪帅), Yuhao Fu(付钰豪), Xin He(贺欣), and Lijun Zhang(张立军)

Citation: Chin. Phys. B, 2021, 30 (**1**): 016402. DOI: 10.1088/1674-1056/abd394
Journal homepage: http://cpb.iphy.ac.cn; http://iopscience.iop.org/cpb

What follows is a list of articles you may be interested in

A high-pressure study of Cr_3C_2 by XRD and DFT

Lun Xiong(熊伦), Qiang Li(李强), Cheng-Fu Yang(杨成福), Qing-Shuang Xie(谢清爽), Jun-Ran Zhang(张俊然)
Chin. Phys. B, 2020, 29 (**8**): 086401. DOI: 10.1088/1674-1056/ab8c3d

Structural transitions in $NaNH_2$ via recrystallization under high pressure

Yanping Huang(黄艳萍), Xiaoli Haung(黄晓丽), Xin Wang(王鑫), Wenting Zhang(张文亭), Di Zhou(周迪), Qiang Zhou(周强), Bingbing Liu(刘冰冰), Tian Cui(崔田)
Chin. Phys. B, 2019, 28 (**9**): 096402. DOI: 10.1088/1674-1056/ab37f8

Calculation of the infrared frequency and the damping constant (full width at half maximum) for metal organic frameworks

M Kurt, H Yurtseven, A Kurt, S Aksoy
Chin. Phys. B, 2019, 28 (**6**): 066401. DOI: 10.1088/1674-1056/28/6/066401

Equation of state of $LiCoO_2$ under 30 GPa pressure

Yong-Qing Hu(户永清), Lun Xiong(熊伦), Xing-Quan Liu(刘兴泉), Hong-Yuan Zhao(赵红远), Guang-Tao Liu(刘广涛), Li-Gang Bai(白利刚), Wei-Ran Cui(崔巍然), Yu Gong(宫宇), Xiao-Dong Li(李晓东)
Chin. Phys. B, 2019, 28 (**1**): 016402. DOI: 10.1088/1674-1056/28/1/016402

Site occupation of doping La^{3+} cations and phase transition in $Na_{0.5}Bi_{0.5}TiO_3$–$BaTiO_3$ solid solution

Liu Li-Ying, Wang Ru-Zhi, Zhu Man-Kang, Hou Yu-Dong
Chin. Phys. B, 2013, 22 (**3**): 036401. DOI: 10.1088/1674-1056/22/3/036401

Temperature-induced phase transition of two-dimensional semiconductor GaTe*

Xiaoyu Wang(王啸宇)[1,†], Xue Wang(王雪)[1,†], Hongshuai Zou(邹洪帅)[1], Yuhao Fu(付钰豪)[2], Xin He(贺欣)[1,‡], and Lijun Zhang(张立军)[1,§]

[1] *State Key Laboratory of Integrated Optoelectronics, Key Laboratory of Automobile Materials of MOE, College of Materials Science and Engineering, Jilin University, Changchun* 130012, *China*

[2] *State Key Laboratory of Superhard Materials, College of Physics, Jilin University, Changchun* 130012, *China*

(Received 8 November 2020; revised manuscript received 23 November 2020; accepted manuscript online 25 November 2020)

GaTe is a two-dimensional III–VI semiconductor with suitable direct bandgap of ∼ 1.65 eV and high photoresponsivity, which makes it a promising candidate for optoelectronic applications. GaTe exists in two crystalline phases: monoclinic (m-GaTe, with space group $C2/m$) and hexagonal (h-GaTe, with space group $P6_3/mmc$). The phase transition between the two phases was reported under temperature-varying conditions, such as annealing, laser irradiation, etc. The explicit phase transition temperature and energy barrier during the temperature-induced phase transition have not been explored. In this work, we present a comprehensive study of the phase transition process by using first-principles energetic and phonon calculations within the quasi-harmonic approximation framework. We predicted that the phase transition from h-GaTe to m-GaTe occurs at the temperature decreasing to 261 K. This is in qualitative agreement with the experimental observations. It is a two-step transition process with energy barriers 199 meV and 288 meV, respectively. The relatively high energy barriers demonstrate the irreversible nature of the phase transition. The electronic and phonon properties of the two phases were further investigated by comparison with available experimental and theoretical results. Our results provide insightful understanding on the process of temperature-induced phase transition of GaTe.

Keywords: two-dimensional semiconductor GaTe, temperature-induced phase transition, first-principles calculation, quasi-harmonic approximation

PACS: 64.60.–I, 71.15.Mb, 81.05.Hd **DOI:** 10.1088/1674-1056/abd394

1. Introduction

In recent years, two-dimensional (2D) semiconductors, bonded through van der Waals forces, have attracted extensive research interests due to their extraordinary properties and potential applications in electronic and optoelectronic devices.[1–5] They have unique layer-dependent electronic properties. III–VIA compound gallium telluride (GaTe) is a 2D layered semiconductor with a moderate direct bandgap of ∼ 1.65 eV[6–8] and a high photoresponsivity for few-layer sheets (10^4 A/W),[9] which render it great potential applications in the field of optoelectronic devices.[10–12] However, current studies on 2D GaTe have obvious limitations. There are two phases of GaTe reported, the monoclinic phase (m-GaTe, space group $C2/m$) and the hexagonal phase (h-GaTe, space group $P6_3/mmc$),[13–16] but current studies are still exclusively restricted to the m-GaTe owing to the difficulty in the fabrication of 2D h-GaTe. Unlike the situation in other III–VIA 2D semiconductor materials, such as GaS, GaSe, and InSe,[17–19] the most stable phase of GaTe under room temperature is the low symmetry monoclinic phase, rather than the high symmetry hexagonal phase.[20]

The phase transition between the monoclinic and hexagonal phases of GaTe was reported experimentally. Gillan *et al.* fabricated h-GaTe using the metal-organic chemical vapor deposition technique. They found that h-GaTe gradually transformed into m-GaTe upon annealing at 500 °C.[15] Yu *et al.* succeeded in driving the GaTe phase transition from h-GaTe to m-GaTe using laser irradiation.[20] Zhao *et al.* obtained h-GaTe by stripping several layers of m-GaTe. They proposed a two-stage transformation mechanism. Firstly, m-GaTe transformed into a tetragonal phase (t-GaTe), then t-GaTe transformed into h-GaTe spontaneously.[21] Both annealing and laser irradiation were accompanied by temperature changes. Gillan *et al.* mentioned that controlling the synthesis temperature affects the lattice structure of the product. Therefore, temperature variation should be the most important factor, which influences the phase transition process of GaTe.

In this paper, we investigated the phase transition of GaTe by using quasi-harmonic approximation (QHA) to estimate the Gibbs free energy.[22] We predicted a phase transition from h-GaTe to m-GaTe when the temperature is lowered to 261 K

*Project supported by the National Natural Science Foundation of China (Grant No. 62004080), Postdoctoral Innovative Talents Supporting Program (Grant No. BX20190143), China Postdoctoral Science Foundation (2020M670834), and Jilin Province Science and Technology Development Program, China (Grant No. 20190201016JC).

†Xiaoyu Wang and Xue Wang contributed equally to this work.

‡Corresponding author. E-mail: xin_he@jlu.edu.cn

§Corresponding author. E-mail: lijun_zhang@jlu.edu.cn

© 2021 Chinese Physical Society and IOP Publishing Ltd

within the QHA method. The calculated results are consistent with the phase transition process from h-GaTe to m-GaTe with the cooling annealing and laser cooling irradiation treatment in the experiments.[15,20] We also used the nudged elastic band (NEB) method[23,24] to estimate the barriers and transition state structures of the phase transition from m-GaTe to t-GaTe and from t-GaTe to h-GaTe. We obtained that the m-GaTe to t-GaTe transition process has a barrier of 199 meV/formula and the t-GaTe to h-GaTe phase transition has a barrier of 288 meV/formula. The relatively high energy barriers demonstrate the irreversible nature of the phase transition, which is consistent with the experimentally observed results. In addition, we further investigated the thermodynamic stable, electronic, and phonon properties of m-GaTe to t-GaTe phases. It was found that the calculated bandgap values and the Raman spectra are in satisfactory agreement with the experimental results, indicating the reliability of our results.

2. Method

We performed first-principles calculations based on density functional theory, as implemented in the Vienna *ab initio* simulation package.[25–27] The electron–core interaction was described by using the projected augmented wave pseudopotentials. The $4s^2 4p^1$ (Ga) and $5s^2 5p^4$ (Te) were treated explicitly as valence electrons. We used the generalized gradient approximation in the Perdew–Burke–Ernzerhof[28] form as the exchange-correlation functional. Structure optimization (including lattice parameters and internal atomic positions) was performed using the conjugate gradient technique[29] until the energy converged to 10^{-6} eV and the force converged to 0.005 eV/Å. A kinetic energy cutoff of 230 eV was used for the wave-function expansion and a grid spacing of $2\pi \times 0.03$ Å^{-1} was used for electronic Brillouin zone integration. To properly take into account the long-range van der Waal (vdW) interactions, after a serious of tests to vdW-optB86b, vdW-optB88, vdW-optPBE, and vdW-DF2 functional, the vdW-optB86b functional was adopted.[30] Since the standard density functional tends to underestimate the band gap of semiconductors, the higher-level hybrid density functional HSE06[31] was used to calculate the electronic structures.[32,33] Spin-orbit coupling was taken into consideration since it is potentially important for electronic structures of heavy p-electron systems. The phase transition barriers were calculated using the NEB method in conjunction with the climbing image method.[23,24,34] Harmonic phonons properties were calculated using the real-space supercell approach as implemented in the PHONOPY code.[35,36] We obtained the temperature dependence of the Gibbs free energy for m-GaTe and h-GaTe by using the QHA theory,[37] which has been successfully used in describing temperature-induced phase transition processes.[22,38–40]

3. Results and discussion

Figures 1(a) and 1(b) show the crystal structures of m-GaTe and h-GaTe, respectively. Both phases have layered structures, with two Ga atoms sandwiched between two Te atoms in each layer. But it is clear that the two structures are quite different in the atom arrangements. In h-GaTe phase, each Ga atom is bonded to one Ga atom and three Te atoms, and the two sublayers present an AA stacking along the perpendicular direction to form bulk, with the weak van der Waals interaction between layers. In contrast, the crystal of m-GaTe demonstrates a distorted layer-structure in which one-third of the Ga–Ga bonds turn from vertical to horizontal towards to the layer plane. The optimized lattice parameters are shown in Table 1, and the corresponding experimental data are also list for reference.[16,41,42] The monoclinic phase m-GaTe with space group $C2/m$ has the lattice parameters of $a = 17.440$ Å, $b = 4.129$ Å, $c = 10.511$ Å, $\alpha = \gamma = 90°$, and $\beta = 103.8°$. The hexagonal phase h-GaTe with space group $P6_3/mmc$ has the lattice parameters of $a = b = 4.106$ Å, $c = 16.918$ Å, $\alpha = \beta = 90°$, and $\gamma = 120°$. Our structural optimization results well agree with the reported experimental values, with an error less than 1%.

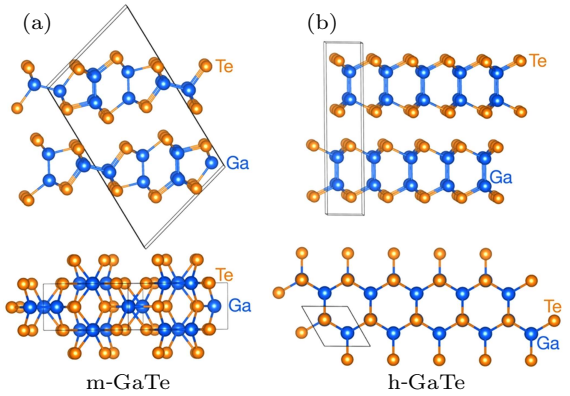


Fig. 1. The side and top views of crystal structures of m-GaTe (a) and h-GaTe (b). The elements of Ga and Te are in blue and brown, respectively.

Table 1. Experimental (Exp.) and calculated (Cal.) lattice parameters (in Å) of m-GaTe and h-GaTe.

		a	*b*	*c*
m-GaTe	Exp.	17.440	4.070	10.460[a]
	Cal.	17.440	4.129	10.511
h-GaTe	Exp.	4.060	4.060	16.956[b]
	Cal.	4.106	4.106	16.918

[a]Refs. [41,42]; [b]Refs. [16,42].

Now, we turn to the phase transition temperature of GaTe. We determined the temperature of phase transition by comparing the Gibbs free energy as a function of temperature at constant pressure. The quasi-harmonic approximation is a phonon-based model of solid-state physics used to describe volume-dependent thermal effects. Within the QHA method,[37] the Helmholtz free energy at temperature T and

equilibrium lattice volume V is defined as

$$F(V,T) = E_{\text{stat}}(V) + F_{\text{el}}(V,T) + F_{\text{vib}}(V,T), \quad (1)$$

where $E_{\text{stat}}(V)$ is the ground state total energy of the crystal which can be obtained by the structural optimization calculation. $F_{\text{el}}(V,T)$ is the thermal electronic contribution to the free energy, which is determined by

$$F_{\text{el}} = E_{\text{el}} - TS_{\text{el}}, \quad (2)$$

the electronic energy E_{el} is given by

$$E_{\text{el}}(V,T) = \int_0^{\infty} n(\varepsilon,V) f(\varepsilon) \varepsilon \, \mathrm{d}\varepsilon - \int_0^{\varepsilon_{\text{F}}} n(\varepsilon,V) \varepsilon \, \mathrm{d}\varepsilon, \quad (3)$$

where $n(\varepsilon,V)$ is the electronic density of states, $f(\varepsilon)$ is the Fermi–Dirac distribution, and ε_{F} is the Fermi level. The electronic entropy S_{el} is defined as

$$S_{\text{el}}(V,T) = -k_{\text{B}} \int_0^{\infty} n(\varepsilon,V) [f(\varepsilon) \ln f(\varepsilon) + (1-f(\varepsilon)) \ln (1-f(\varepsilon))] \mathrm{d}\varepsilon. \quad (4)$$

$F_{\text{vib}}(V,T)$ is the phonon contribution to the free energy, which is determined by

$$F_{\text{vib}} = \frac{1}{2} \sum_{\boldsymbol{q}\lambda} \hbar \omega_{\boldsymbol{q}\lambda}(V) + k_{\text{B}} T \times \sum_{\boldsymbol{q}\lambda} \ln \left[1 - \exp \left(-\frac{\hbar \omega_{\boldsymbol{q}\lambda}(V)}{k_{\text{B}} T} \right) \right], \quad (5)$$

where $\boldsymbol{q}$ is all wave vectors and λ is all three phonon branches in the first Brillouin zone. k_{B} is the Boltzmann constant, $\hbar$ is the reduced Planck constant, and $\omega_{\boldsymbol{q}\lambda}(V)$ is the frequency of the phonon. Then the Gibbs free energy is obtained by minimizing the free energy,

$$G(T,P) = \min_V [F(V,T) + PV], \quad (6)$$

where $\min_V$[function of V] means to find the unique minimum value in the brackets by changing the volume. Figure 2(a) shows the curves of the Gibbs free energy with respect to temperature of m-GaTe and h-GaTe. The curve intersects at 261 K. Therefore, we proved the possibility of a temperature-induced phase transition between the two phases and predicted the theoretical phase transition temperature of 261 K.

We further obtained the trend of volume change with temperature, as shown in Fig. 2(b). The volume of m-GaTe is smaller than that of h-GaTe over the studied temperature range. Meanwhile, the thermal expansion coefficient of m-GaTe is higher. Therefore, in the phase transition process from m-GaTe to h-GaTe, the crystal lattice of h-GaTe suffers growing compressive stress during the nucleation and growth process. As a result, the phase transition requires a greater driving force, and the actual phase transition temperature of the heating process might be higher than the theoretical phase transition temperature. The current analysis also provides a new perspective for understanding the spontaneous phase transition from m-GaTe to h-GaTe caused by the exfoliating process: when the bulk GaTe is exfoliated into layered GaTe, the stress is released. According to the relationship of Gibbs free energy described above, there will be a spontaneous phase transition from m-GaTe to h-GaTe under room temperature.

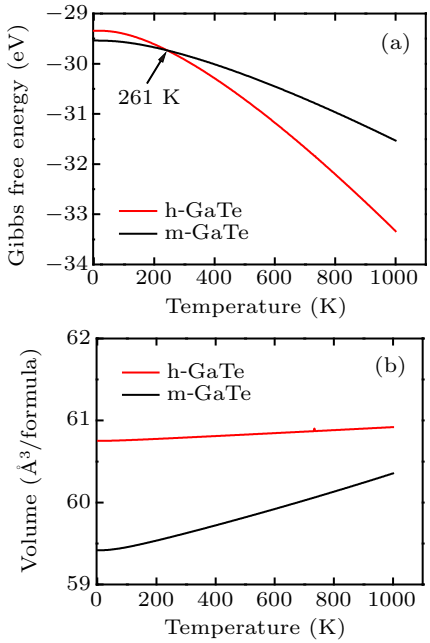


Fig. 2. (a) Gibbs free energy versus temperature of h-GaTe (red line) and m-GaTe (black line) curve. (b) Volume versus temperature of h-GaTe (red line) and m-GaTe (black line).

In order to have an in-depth understanding of the phase transition of GaTe, we further calculated the energy barrier to obtain the energy required to accomplish the phase transition. We adopted a two-step phase transition process mechanism, which has been reported by Zhao *et al.*[21] The structure evolution and energy barriers have been identified by using NEB method with five and eight images as intermediate states for the phase transition process from m-GaTe to t-GaTe and from t-GaTe to h-GaTe, respectively. The results are shown in Fig. 3. Both m-GaTe and h-GaTe have a layered structure, which means that the phase transformation occurs within the layers. The first step is the phase transition from m-GaTe to t-GaTe. In this process, the Ga–Ga bonds parallel to the layers are reversed and transformed into positions perpendicular to the layers. The process is accompanied by the breakage of the original Ga–Te bonds and the generation of new Ga–Te bonds. The transition state structure of the first step corresponds to the structure whose Ga–Te bonds are between the bond breaking and bond formation processes. The second step is the movement of the entire layer of Te atoms, resulting in the phase transition from t-GaTe to h-GaTe. The transition state structure of the second step corresponds to the structure whose Te

atoms move to the intermediate critical positions between the Ga atoms. The barrier of the first process is 199 meV/formula and that of the second process is 288 meV/formula. Previous studies have shown that the phase transition barrier of $\sim$ 300 meV/formula is sufficiently large to demonstrate the stability of the phase transition product of indium selenide and tungsten ditelluride.[43,44] Therefore, the relatively high energy barriers ensure that the phase transition of GaTe is irreversible. We note that the phase transition from m-GaTe to t-GaTe is accompanied by bond formation and bond breaking, but the barrier is lower than that of the phase transition from t-GaTe to h-GaTe. This is due to the considerable atom movement in the t-GaTe to h-GaTe transition process, even half of the Te atoms are involved in the movement.

Then we focus on the electronic properties of m-GaTe and h-GaTe phases to evaluate their application potentials for photovoltaics. Figures 4(a) and 4(b) show the calculated orbital projected band structures for m-GaTe and h-GaTe. It can be seen that m-GaTe is a direct bandgap semiconductor with a bandgap of 1.449 eV which is close to the experimental value of 1.65 eV.[45,46] The h-GaTe is an indirect bandgap semiconductor with an indirect bandgap of 0.608 eV and a direct bandgap of 1.089 eV. The experimentally prepared h-GaTe film is an indirect bandgap semiconductor with the bandgap value of 1.06 eV, which is larger than our calculated result.[47] Both the conduction band minimum (CBM) and the valence band maximum (VBM) are mainly associated with the Te p states and exhibit strong band edge dispersion, thus inferring that the effective masses of the carriers should be small. Indeed, the effective masses of electron (m_e^*) and hole (m_h^*) in m-GaTe ($m_e^* = 0.11m_0$, $m_h^* = 0.28m_0$) and h-GaTe ($m_e^* = 0.12m_0$, $m_h^* = 0.18m_0$) are much smaller than the free electron mass m_0 in our calculation, which is favorable for the migration of electrons and holes. They have been predicted to have good carrier transport properties. It can be seen that the m-GaTe is promising for applications in photovoltaic devices due to its suitable bandgap value, direct bandgap nature, and good carrier transport property.

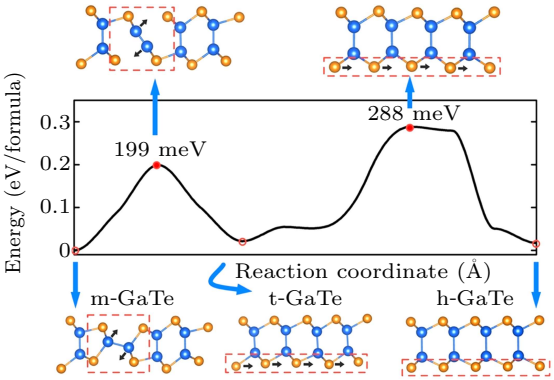


Fig. 3. Phase transition barriers from m-GaTe to h-GaTe and schematic representation of the bond and atom rearrangement in the phase transition process.

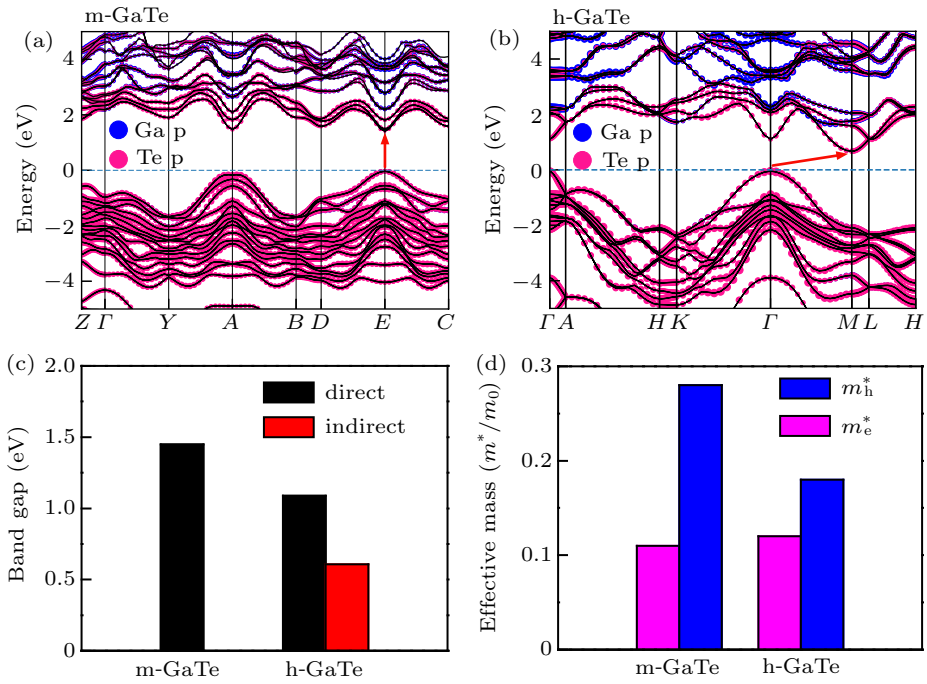


Fig. 4. (a), (b) Calculated orbital projected electronic band structures for m-GaTe (a) and h-GaTe (b). Red and blue colors represent projections onto constituting orbital species Te p and Ga p. (c) Calculated bandgap results by using HSE06 + SOC functional. (d) Calculated effective masses of electron (m_e^*) and hole (m_h^*).

Figures 5(a) and 5(b) show the calculated phonon dispersion curves of m-GaTe and h-GaTe, which exhibit no imaginary modes in the whole Brillouin region, thus indicating that the two phases are kinetically stable. Figures 5(c) and 5(d) show our calculated Raman spectra, and the corresponding experimental data from previous works. The most active two peaks are 109.04 cm^{-1} and 114.85 cm^{-1} for m-GaTe in our calculation. They are in good agreement with the experimental measurements

of 109 cm^{-1} and 115 cm^{-1} for freshly cleaved GaTe (Exp. 1).[48] Due to oxidization, the m-GaTe Raman peaks decrease whereas the new peaks at wavenumbers 123 cm^{-1} and 140 cm^{-1} become prominent over time under ambient condition (Exp. 2).[49] However, previous works insisted on the two peaks belonging to intrinsic Raman peaks of h-GaTe.[20,49,50] In our calculated results for h-GaTe, the most active peak is 96.75 cm^{-1}. The Raman spectra need more experimental and theoretical approaches for further clarification.

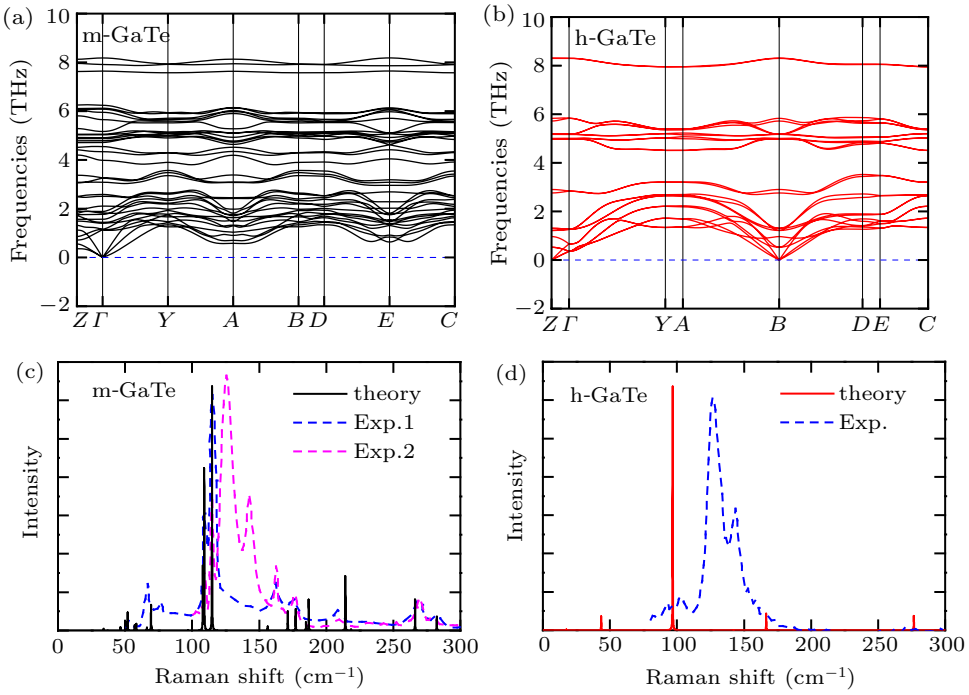


Fig. 5. Calculated phonon dispersion and Raman spectra of (a), (c) m-GaTe and (b), (d) h-GaTe. Here theory is our result, compared with experiment results from previous reports (Exp. 1,[48] Exp. 2,[49] Exp.[20]).

4. Conclusion and perspectives

By using first-principles energetic and phonon calculations within the quasi-harmonic approximation framework, we investigated the temperature-induced phase transition process in two-dimensional semiconductor GaTe. We predicted that the phase transition from h-GaTe to m-GaTe will occur at the temperature decreasing to 216 K. Our results are consistent with the phase transition condition from h-GaTe to m-GaTe observed in the experiments, such as the cooling process during annealing and laser irradiation. Based on the previously reported two-step phase transition process, we used the nudged elastic band method to calculate the phase transition barriers and investigate the corresponding transition state structures. The m-GaTe to t-GaTe phase transition barrier is 199 meV/formula and the t-GaTe to h-GaTe phase transition barrier is 288 meV/formula. The large phase transition barriers demonstrate the irreversible nature of the phase transition. The structure evolution in the phase transition process indicated that the bond broken is responsible for the high energy barriers. The electronic and phonon properties of the two phases were further investigated by comparison with available experimental and theoretical results. The m-GaTe is a direct bandgap semiconductor with a gap of 1.449 eV, which is close to the experimental value. The h-GaTe is an indirect bandgap semiconductor whose fundamental energy bandgap is 0.608 eV (0.48 eV lower than the direct bandgap). Our calculated Raman spectra are in general agreement with the experimentally measured data. This work provides insightful understanding on the process of temperature-induced phase transition of GaTe.

Acknowledgments

We acknowledge stimulating discussions with Prof. Xuetao Gan (Northwestern Polytechnical University). Calculations were performed in part at the high-performance computing center of Jilin University.

References

[1] Zhao X G, Shi Z, Wang X, Zou H, Fu Y and Zhang L 2020 *InfoMat*
[2] Wang Z, Zhao D, Yu S, Nie Z, Li Y and Zhang L 2019 *Progress in Natural Science: Materials International* **29** 316
[3] Shi Q, Dong B, He T, Sun Z, Zhu J, Zhang Z and Lee C 2020 *InfoMat* **2** 1131
[4] Yu F, Hu M, Kang F and Lv R 2018 *Progress in Natural Science: Materials International* **28** 563
[5] Huang B Q, Zhou T G, Wu D X, Zhang Z F and Li B K 2019 *Acta Phys. Sin.* **68** 246301 (in Chinese)
[6] Çınar K, Çaldıran Z, Coşkun C and Aydoğan Ş 2014 *Thin Solid Films* **550** 40
[7] Pal S and Bose D N 1996 *Solid State Commun.* **97** 725
[8] Wang Y, Tian F, Li D, Duan D, Xie H, Liu B, Zhou Q and Cui T 2019 *Chin. Phys. B* **28** 056104

[9] Liu F, Shimotani H, Shang H, Kanagasekaran T, Zolyomi V, Drummond N, Fal'ko V I and Tanigaki K 2014 *ACS Nano* **8** 752
[10] Wang F, Wang Z, Xu K, Wang F, Wang Q, Huang Y, Yin L and He J 2015 *Nano Lett.* **15** 7558
[11] Yang S, Wang C, Ataca C, Li Y, Chen H, Cai H, Suslu A, Grossman J C, Jiang C, Liu Q and Tongay S 2016 *ACS Appl. Mater. Interfaces* **8** 2533
[12] Kang J, Sangwan V K, Lee H S, Liu X and Hersam M C 2018 *ACS Photon.* **5** 3996
[13] Kolesnikov N N, Borisenko E B, Borisenko D N and Timonina A V 2013 *Journal of Crystal Growth* **365** 59
[14] Balitskii O A, Jaeckel B and Jaegermann W 2008 *Phys. Lett. A* **372** 3303
[15] Gillan E G and Barron A R 1997 *Chem. Mater.* **9** 3037
[16] Semiletov S A and Vlasov V A 1963 *Kristallografiya* **8** 877
[17] Finkman E and Rizzo A 1974 *Solid State Commun.* **15** 1841
[18] Chevy A, Kuhn A and Martin M S 1977 *Journal of Crystal Growth* **38** 118
[19] Shen G, Chen D, Chen P C and Zhou C 2009 *ACS Nano* **3** 1115
[20] Yu Y, Ran M, Zhou S, Wang R, Zhou F, Li H, Gan L, Zhu M and Zhai T 2019 *Adv. Funct. Mater.* **29** 1901012
[21] Zhao Q, Wang T, Miao Y, Ma F, Xie Y, Ma X, Gu Y, Li J, He J, Chen B, Xi S, Xu L, Zhen H, Yin Z, Li J, Ren J and Jie W 2016 *Phys. Chem. Chem. Phys.* **18** 18719
[22] McKinley J L and Beran G J O 2019 *J. Chem. Theory Comput.* **15** 5259
[23] Henkelman G, Uberuaga B P and Jónsson H 2000 *The Journal of Chemical Physics* **113** 9901
[24] Henkelman G and Jónsson H 2000 *The Journal of Chemical Physics* **113** 9978
[25] Kresse G and Furthmüller J 1996 *Computational Materials Science* **6** 15
[26] Kresse G and Furthmüller J 1996 *Phys. Rev. B* **54** 11169
[27] Wang X, Huang S X, Luo H, Deng L W, Wu H, Xu Y C, He J and He L H 2019 *Acta Phys. Sin.* **68** 187301 (in Chinese)
[28] Perdew J P, Burke K and Ernzerhof M 1996 *Phys. Rev. Lett.* **77** 3865
[29] Vetterling W T, Teukolsky S A, Press W H and Flannery B P 1989 *Numerical recipes* (New York: Cambridge University Press)
[30] Klimeš J, Bowler D R and Michaelides A 2009 *J. Phys.: Condens. Matter* **22** 022201
[31] Heyd J, Scuseria G E and Ernzerhof M 2003 *J. Chem. Phys.* **118** 8207
[32] Liu Z, Na G, Tian F, Yu L, Li J and Zhang L 2020 *InfoMat* **2** 879
[33] Yin W, Wen B, Ge Q, Wei X, Teobaldi G and Liu L 2020 *Progress in Natural Science: Materials International* **30** 128
[34] Chen A, Zhang X and Zhou Z 2020 *InfoMat* **2** 553
[35] Tang X, Gu J, Shang J, Chen Z and Kou L 2020 *InfoMat*
[36] Wang Z, Jiang C, Fang Q, Liu F, Liu B, Fan T, Ma L and Tang P 2020 *Progress in Natural Science: Materials International* **30** 424
[37] Wei Y K, Ge N N, Chen X R, Ji G F, Cai L C and Gu Z W 2014 *J. Appl. Phys.* **115** 124904
[38] Wang R, Wang S and Wu X 2011 *Phys. Scr.* **83** 065707
[39] McKinley J L and Beran G J O 2018 *Faraday Discuss.* **211** 181
[40] Kaur K and Kumar R 2016 *Progress in Natural Science: Materials International* **26** 533
[41] Hu S Z and Parthé E 2004 *Jiegou Huaxue* **23** 11
[42] Shenoy U S, Gupta U, Narang D S, Late D J, Waghmare U V and Rao C N R 2016 *Chemical Physics Letters* **651** 148
[43] Sun Y, Li Y, Li T, Biswas K, Patanè A and Zhang L 2020 *Adv. Funct. Mater.* **30** 2001920
[44] Lu P, Kim J S, Yang J, Gao H, Wu J, Shao D, Li B, Zhou D, Sun J, Akinwande D, Xing D and Lin J F 2016 *Phys. Rev. B* **94** 224512
[45] Brebner J, Fischer G and Mooser E 1962 *Journal of Physics and Chemistry of Solids* **23** 1417
[46] Tatsuyama C, Watanabe Y, Hamaguchi C and Nakai J 1970 *J. Phys. Soc. Jpn.* **29** 150
[47] Vega J J F 2017 *Bandgap engineering of gallium telluride* (Berkeley: University of California)
[48] Susoma J, Lahtinen J, Kim M, Riikonen J and Lipsanen H 2017 *AIP Advances* **7** 015014
[49] Huang S, Tatsumi Y, Ling X, Guo H, Wang Z, Watson G, Puretzky A A, Geohegan D B, Kong J, Li J, Yang T, Saito R and Dresselhaus M S 2016 *ACS Nano* **10** 8964
[50] Bae C J, McMahon J, Detz H, Strasser G, Park J, Einarsson E and Eason D B 2017 *AIP Advances* **7** 035113